

An optimised chemisorption cycle for power generation using low grade heat



Huashan Bao, Zhiwei Ma*, Anthony Paul Roskilly

Sir Joseph Swan Centre for Energy Research, Newcastle University, Newcastle upon Tyne NE1 7RU, UK

HIGHLIGHTS

- A novel advanced resorption power generation cycle with reheating process.
- The optimal desorption temperature needs to be identified for maximum work output.
- Continuous waste heat recovery and work output with single-effect cycle.
- Reheating process improved the total work output by 10–600%.
- Considerable cooling output without compromising maximum work output.

ARTICLE INFO

Article history:

Received 17 March 2016
 Received in revised form 14 May 2016
 Accepted 17 June 2016
 Available online 28 June 2016

Keywords:

Chemisorption power generation
 Reheat
 Optimal desorption temperature
 Low grade heat
 Refrigeration

ABSTRACT

The integration of chemisorption cycle with turbine/expander opens up enormous opportunities of recovering low grade heat to meet different energy demands including heating, cooling and power generation. In the present study, a novel advanced resorption power generation (RPG) cycle with reheating process has been proposed for the first time to significantly improve the thermal efficiency and exergy efficiency of the basic RPG cycle. Such a reheating concept is built on the premise of chemisorption monovariant characteristic and identification of the optimal desorption temperature aiming at producing the maximum work output under the given working conditions. The identified optimal desorption temperature might be lower than the available heat source temperature, and the desorbed ammonia vapour is subsequently reheated to the heat source temperature before it undergoes vapour expansion for power generation. This study explored the potential of the proposed advanced RPG cycle and investigated the system performance using three representative resorption sorbent pairs, including manganese chloride – sodium bromide, manganese chloride – strontium chloride, and strontium chloride – sodium bromide, all with ammonia as the refrigerant. The application of reheating concept can improve the total work output of RPG cycle by 10–600%, depending on different sorbent pairs and different heat source temperatures studied in this work, e.g., when the heat source temperature is at 200 °C, the thermal efficiency is increased by 1.4–4.5 times and the exergy efficiency is boosted by 2.0–8.3 times. Another valuable merit of the proposed RPG cycle is that there is a great potential of considerable amount of additional cooling output without compromising the maximum work output, leading to further improvement of system efficiency. Compared to other bottoming cycles for power generations, the proposed advanced RPG cycle exhibits the highest thermal efficiency when the heat source temperature is between 120 °C and 200 °C.

© 2016 The Authors. Published by Elsevier Ltd. This is an open access article under the CC BY license (<http://creativecommons.org/licenses/by/4.0/>).

1. Introduction

There have been massive researches and developing efforts on sorption technology, including absorption and adsorption cycles for air conditioning and refrigeration [1], heat pump and heat transformation [2,3], dehumidification and desalination [4], energy

storage [5], etc. Although the current sorption technology encounters challenges not just from technical aspect but also in relation to economical issue as it is trudging towards the fiercely competitive and crucial commercial market, above all different specific reasons, the prevailing argument in favour of sorption systems is the potential of using environmentally friendly refrigerants and harnessing low grade heat, leading to energy efficiency improvement and CO₂ emission reduction [1,2]. Ever since Maloney and Robertson [6] as the first pioneer studied ammonia–water based absorption

* Corresponding author.

E-mail address: zhiwei.ma@newcastle.ac.uk (Z. Ma).

Nomenclature

c_p	heat capacity (J/(kg K))
COP	coefficient of performance (–)
E	exergy (J)
h	enthalpy (J/kg)
ΔH_r	chemisorption enthalpy (J/mol (NH ₃))
m	mass (kg)
M	molar mass (g/mol)
P	pressure (Pa)
Q	heat (J)
ΔS_r	chemisorption entropy (J/(mol K))
T	temperature (K)
ΔT	temperature difference (K)
W	work (J)
Δx	global conversion of chemisorption (–)

Greeks

η	efficiency (–)
--------	----------------

Subscripts

a	ambient
des	desorption
EG	expanded graphite
en	energy
eq	equilibrium
ex	exergy
input	input
NH ₃	ammonia
opt	optimal
ref	refrigeration
reheat	reheat
s	source
salt	salt
sen	sensible
w	work

power generation cycle, and later on the improvement by the Kalina cycle [7] justified the further efforts on this promising technology, more and more researches have been inspired to develop power generation or cogeneration of power and cooling through ammonia-based heat powered cycles, such as the growing family of Kalina cycle systems [8], Goswami cycles [9], absorption power/cooling combined cycles [10,11], and salt-ammonia chemisorption power generation cycles [12–14].

A few demonstration power plants as well as a couple of commercial ones have been built and implemented based on Kalina cycles across the world, driven by geothermal energy, or solar thermal energy or industrial waste heat [15,16]. With fast-progressing technique in the relevant fields, in the near future it can be expected that Kalina power generation system will enter the real market and exhibit its excellent competitiveness. Compared to absorption based Kalina cycles, the salt-ammonia chemisorption cycle is a discontinuous and less stable process with some shortcomings like heat and mass transfer issue and performance degradation concern due to the involved chemicals. Nevertheless, chemisorption cycle features simpler configuration and diverse sorbents to be suitable for a wider range of operational conditions. On the other hand, Kalina cycles require superheating process to tackle the drawback of the ammonia being a wet fluid; additionally, sufficiently low condensing temperature is necessary to assure the power generation driven by low grade heat, for example, the geothermal power plant in Húsavík, one of successful Kalina cycle power plants in the world so far, is using around 5 °C cooling water melted from the snow-covered mountain [15]. From this point of view, chemisorption power generation cycle has the commendable advantage of more resistance to the limitation of ammonia being wet due to the chemical reaction equilibrium, leading to the potential of more productive generation driven by low grade heat [14,17].

Ammonia-based chemisorption power generation cycle has an expander mounted in between two vessels, i.e., one sorbent reactor and the other one condenser/evaporator. The pipeline arrangement allows reversible flow direction between these two vessels all passing through the expander to achieve power generation in both half-cycles. It benefits from the thermodynamic equilibrium of chemical reaction so that the desorbed ammonia is already at superheated vapour state, suggesting the wet fluid limitation can be significantly alleviated. As an alternative type of chemisorption, resorption system has two sorbent reactors as each reactor contains one kind of reactant salt [18,19]. In a resorption power gen-

eration (RPG) cycle, the inlet pressure of the expander is desorption pressure in the sorbent reactor at the upstream of the expander, while the backpressure is adsorption pressure in the other sorbent reactor. Thus there in fact potentially exists a larger pressure ratio to drive the expander rotation compared to conventional one-sorbent chemisorption, in other word, the RPG cycle can create even more favourable atmosphere for ammonia expansion [12,13]. Nevertheless, this great potential cannot be fully harnessed due to again the wet fluid feature and the dryness requirement for the healthy operation of the expander. As reported in the previous work [17], the utilisation efficiency (the ratio value of the actual expansion ratio over the available pressure ratio) is no more than 30%, and the worse thing is that this utilisation efficiency declines with the increase of heat source temperature.

In this work, thermodynamic analysis and optimisation of RPG cycle has been conducted in order to gain better knowledge and explore maximum benefits, as a result an advanced RPG cycle with optimal arrangement of thermal energy supply was proposed for the first time to address the foregoing issue, aiming to mitigate the limitation of ammonia being wet so that to optimally harness the great power generation potential of RPG cycles. The performance improvement compared to the basic RPG cycle was investigated in detail through three representative resorption sorbent pairs, MnCl₂–NaBr, MnCl₂–SrCl₂, and SrCl₂–NaBr. The efficacy of power and cooling cogeneration of the proposed advanced RPG cycle was also evaluated. Moreover, the comparison with other bottoming cycles, e.g., organic Rankine cycle, stirling cycle and thermal-electric cycle, was conducted to discuss the competitiveness of this advanced RPG cycle.

2. Working principles

2.1. Thermodynamic principle of RPG cycle

A single-effect ammonia-based chemisorption refrigeration cycle (termed as conventional cycle in the context) consists of one solid sorbent reactor, one condenser/evaporator. A resorption cycle substitutes one secondary reactor containing a secondary solid sorbent for the condenser/evaporator in the conventional cycle. Generally, a resorption heat pump cycle uses two different salts to group up an sorbent pair, e.g., MnCl₂–NaBr pair, and they are differentiated by their equilibrium temperatures at the same working pressure so as one is called high temperature sorbent

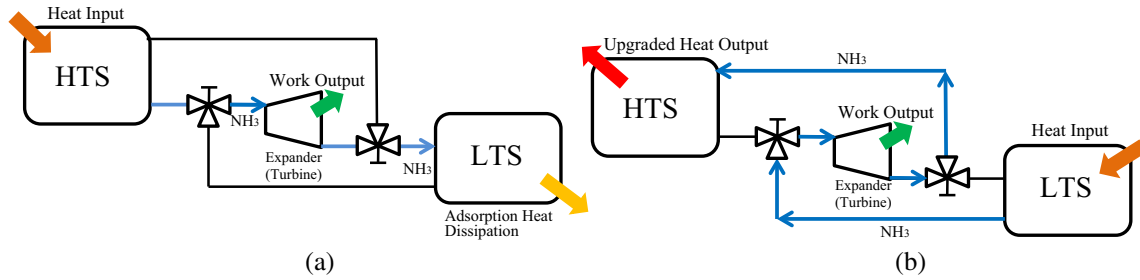


Fig. 1. Basic RPG cycle, (a) first half-cycle: heat input to HTS and power generation; (b) second half-cycle: heat input to LTS, power generation and potentially heat upgrade.

(HTS) while the other one is low temperature sorbent (LTS) [18,19]. A basic RPG cycle is schematised in Fig. 1 with the typical configuration of a single-effect resorption cycle (two sorbent reactors) while an expander is positioned in between two reactors. The ammonia vapour dissociated at high pressure and high temperature from one reactor is headed to the expander where the mechanical power is generated before it ends up being adsorbed by the other reactor. As the first and second half-cycles being illustrated by Fig. 1(a) and (b) respectively, a RPG cycle can realise continuous recovery of waste heat from uninterrupted industrial processes for power output in both half-cycles, like quasi-continuous output. There is also a potential to generate considerable amount of upgraded heat in the second half-cycle if the exothermal synthesis occurs between the HTS and the expansion exhaust at high pressure.

The thermodynamic processes of RPG cycles are plotted in Clapeyron diagram of Fig. 2, exemplified by $\text{MnCl}_2\text{-NaBr}$ pair and $\text{MnCl}_2\text{-SrCl}_2$ pair. In the first half-cycle, HTS reactor is supplied with heat (point A in Fig. 2) to desorb ammonia vapour at high temperature and high pressure. Because of the pressure and temperature, the ammonia vapour has the potential to expand through the expander with work output (process A–B, isentropic expansion), and subsequently the exhausted ammonia vapour is adsorbed by LTS at heat sink temperature T_a (point C), therefore, the vapour expansion is subject to the LTS adsorption pressure at T_a as the backpressure. In the second half-cycle, LTS reactor is provided with the same heat source and undertakes temperature raise (C–D) and endothermic decomposition while HTS reactor is cooled at the heat sink temperature. Because LTS has higher equilibrium pressure than HTS does when at the same temperature, the released ammonia vapour from LTS reactor is at much higher pressure (point D) than that in the first half-cycle, and again the vapour passes through the expander for the second generation of mechan-

ical power. The backpressure of this second expansion is HTS adsorption pressure at the heat sink temperature, and it can be as low as the vacuum level, suggesting a favourable environmental condition for vapour expansion. On the other hand, the ammonia expansion is limited by the condition of vapour dryness for healthy and durable expander operation, therefore it is assumed that the expansion terminates once the working fluid reaches its saturation as depicted by the curve D–E in Fig. 2. Eventually, the sum of process A–B and D–E represents the total potential work output by one complete RPG cycle. The RPG cycle using $\text{MnCl}_2\text{-SrCl}_2$ pair has more power output than that using $\text{MnCl}_2\text{-NaBr}$ pair in the first half-cycle ($A1B1 < A2B2$, in Fig. 2), due to the larger pressure ratio in $\text{MnCl}_2\text{-SrCl}_2$ RPG cycle. In the second half-cycle, the work output by the $\text{MnCl}_2\text{-NaBr}$ RPG cycle is heavily hindered by the ammonia saturation condition, in spite of greater pressure ratio than that of the $\text{MnCl}_2\text{-SrCl}_2$ pair. Ultimately, the $\text{MnCl}_2\text{-SrCl}_2$ pair is very likely to outproduce the $\text{MnCl}_2\text{-NaBr}$ pair ($A1B1 + D1E1 < A2B2 + D2E2$) under the same conditions of heat source and heat sink.

Since the vapour expansion halts at relatively high pressure (point E) in the second half-cycle, the exothermal synthesis between the exhausted ammonia and HTS sorbent occurs at relatively high equilibrium temperature (point F), which realizes the thermal energy upgrading (heat transformation). If the heat upgrade is desired as much as possible, the released ammonia can be absorbed directly by the HTS reactor at a higher pressure (at point E') without expansion process. Certainly, the energy output shares (heat or power) can be balanced according to the specific demand by adjusting the expansion ratio. For example, the slightly modified cycle D2–E2'–F2' in dash-dot line in Fig. 2 compromises some work output for larger heat upgrading degree.

2.2. Advanced RPG cycle

A reheating process is proposed to overcome the barriers of ammonia being wet fluid and to maximise the realisation of the available pressure ratio in RPG cycle. This reheating method depicts an extra heating of the desorbed ammonia vapour before it expands, and the reheating condition is relatively sophisticated because it is on the premise of the identification of the optimal desorption temperature.

Fig. 3 displays the augment of power generation based on the desorption-expansion of NaBr ammoniate with reheating process when it couples with SrCl_2 . Two main restrictions for the expansion in RPG cycle, i.e. ammonia saturation condition and the backpressure (adsorption pressure at the downstream of the expander), are graphically translated in the Clapeyron diagram as the states of the expansion exhaust must fall into the grey-marked region in Fig. 3(a), where the pressure is higher than the backpressure but lower than the ammonia saturation pressure. Owing to the monovariant characteristic of chemisorption cycle, desorption temperature/pressure can be adjusted before isobaric reheating process so that to acquire the maximum work output. With a given heat

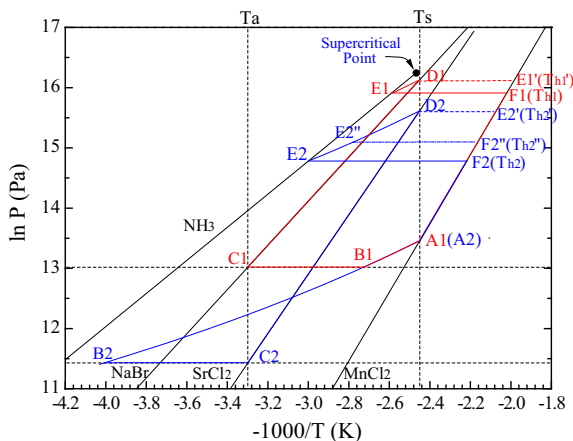


Fig. 2. Clapeyron diagram of basic RPG cycles, using $\text{MnCl}_2\text{-NaBr}$ and $\text{MnCl}_2\text{-SrCl}_2$ sorbent pairs as examples.

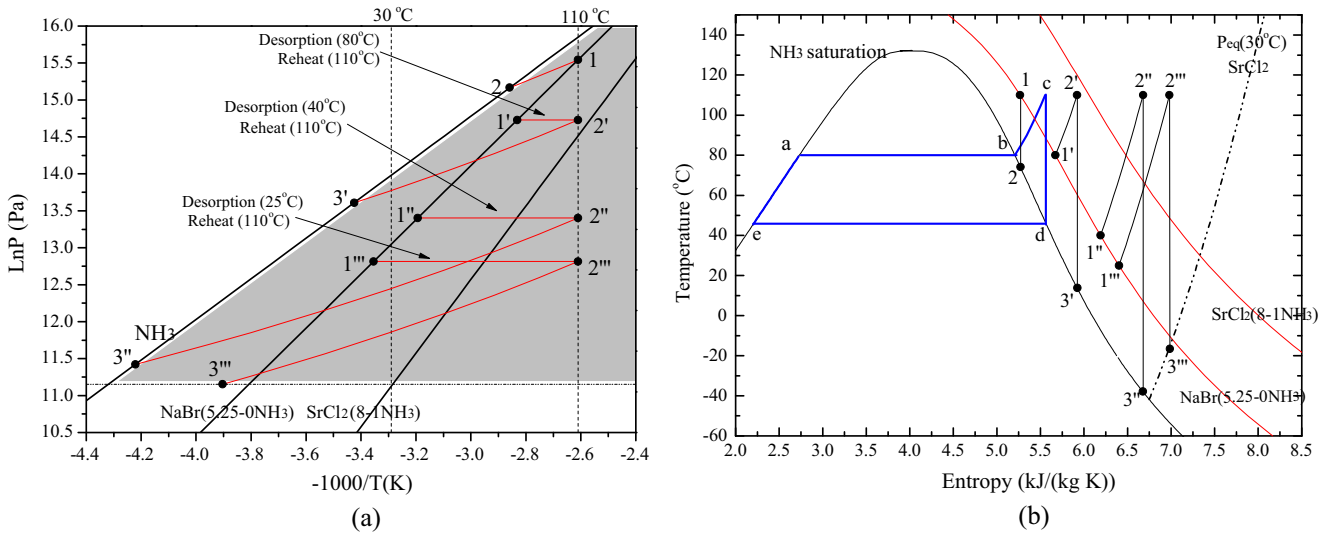


Fig. 3. Reheating method to improve the power generation in advanced RPG cycle, (a) Clapeyron P-T diagram and (b) T-S diagram.

source, there are more than one way to arrange desorption and reheating, resulting in different quantity of work output. The exemplified four different desorption processes in Fig. 3(a) use temperatures 110 °C, 80 °C, 40 °C, 25 °C, respectively, the desorbed ammonia vapour is subsequently reheated isobarically to the heat source temperature of 110 °C. It is evident that the isentropic work output firstly increases with the decreasing desorption temperature ($1-2 < 2'-3' < 2''-3''$) due to the enlarged deviation of the state of the expander inlet ammonia vapour from the ammonia saturation line; and then the work output decreases as reducing the desorption temperature further ($2''-3'' > 2'''-3'''$) because of the limitation of the adsorption equilibrium pressure of SrCl₂. Thus,

it can speculate that there exists an optimal point of desorption temperature yielding the maximum work output with a given heat source temperature. The same conclusion can also be obtained from the T-S diagram as shown in Fig. 3(b).

The reheating process can be effectively implemented with rational management of thermal energy utilisation at different temperature levels. One vivid and common situation in industrial processes is that there are several streams of waste heat available at different temperature, in this instance, the selection and arrangement of waste heat separately for desorption and reheating process can be conducted, as shown in Fig. 4(a), rather than blindly picking the heat source at the highest temperature for desorption

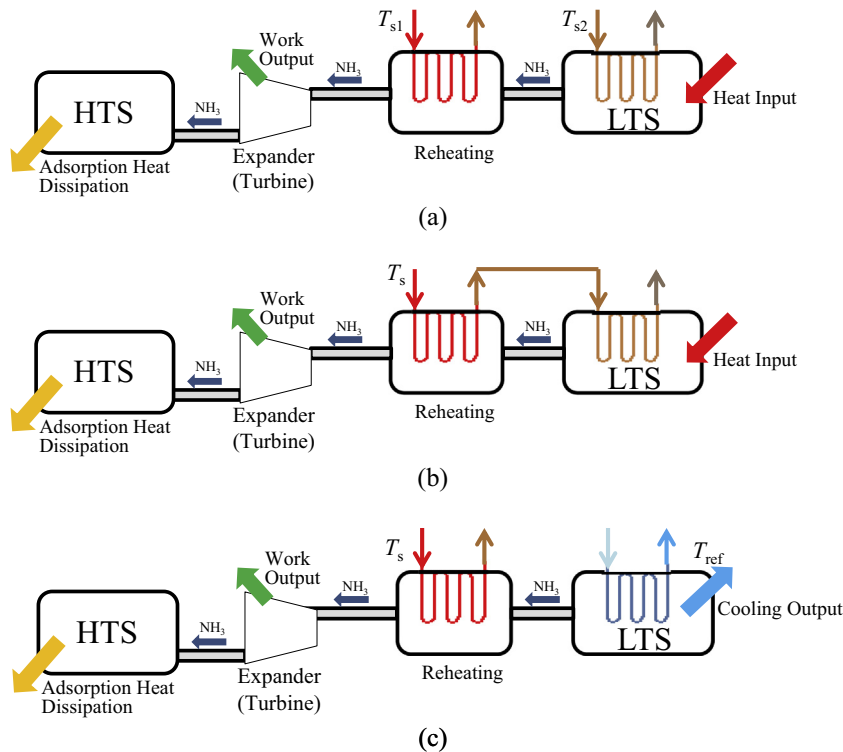
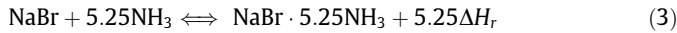
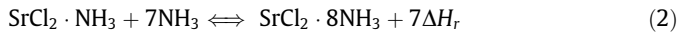
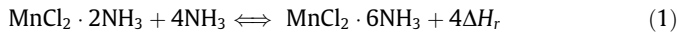


Fig. 4. Different arrangements of advanced RPG cycle, (a) two heat sources at different temperatures; (b) single heat source; (c) single heat source, LTS desorption at low temperature with cooling output.

process. If there is only one single heat source at certain temperature, the heat source should serve the reheating heat exchanger prior to the desorption reactor if the identified optimal desorption temperature is lower than heat source temperature, as illustrated in Fig. 4(b), meanwhile the heat exchange area and flow rate of the heat transfer fluid should be carefully determined to achieve the designed condition. Alternatively, if the optimal desorption temperature turns out to be lower than the ambient temperature, the cooling energy can be produced by the decomposition at lower temperature as shown in Fig. 4(c). It should be noted that the “heat source temperature” in the following sections unnecessarily represents desorption temperature but the available highest temperature heat source.

3. Analytical methodology

The cycle performance with the heat source between 40 °C and 200 °C and heat sink temperature at 25 °C was evaluated through the following equations with physical and chemical property parameters of sorbent salts summarised in Table 1. The ammonia real gas properties used in the calculation was provided by NIST REFPROP 9.1. The resorption salt pairs were grouped between three typical salts, MnCl₂, SrCl₂ and NaBr, as the coordination reaction of each salt ammoniate with ammonia can be formulated as Eqs. (1)–(3).



Expanded graphite was used as porous supporting matrix to be mixed with salt ammoniate as the composite sorbent. The mass ratio of graphite and salt was 1:3 and the bulk density of the composite sorbent was 450 kg/m³. It has been reported that such a composite sorbent had an enhanced thermal conductivity of 1.7–3.1 W/(m K) and permeability in the magnitude of 10⁻¹²–10⁻¹¹ m², depending on different ammonia uptakes [20], thus the mass transfer limitation within the composite sorbent could be ignored at relatively high working pressure [21].

The sensible heat, the total heat input for desorption process and the corresponding exergy were calculated by Eqs. (4)–(6), where the heat capacity of the salt ammoniate was estimated as the sum of heat capacity of the salt and that of ammonia in a condensed phase which was confined within the solid ammoniate [22]. The sensible heat consumed by the metal reactor was not taken into account in current generic calculation.

$$\begin{aligned} Q_{\text{sen}} &= \int_{T_1}^{T_2} \sum_{i=1}^3 (m \cdot c_p(T))_i dT \\ &= \int_{T_1}^{T_2} \left[(m \cdot c_p(T))_{\text{EG}} + (m \cdot c_p(T))_{\text{salt}} + (m \cdot c_p(T))_{\text{NH}_3} \right] dT \end{aligned} \quad (4)$$

$$Q_{\text{input}} = Q_{\text{sen}} + \Delta H_r \cdot \Delta x \quad (5)$$

$$E_{\text{input}} = (1 - T_a/T_s) Q_{\text{input}} \quad (6)$$

The consumed energy and the corresponding exergy in the desorption-reheating process were calculated by Eqs. (7)–(10):

$$\begin{aligned} Q_{\text{sen,opt}} &= \int_{T_1}^{T_{\text{opt}}} \sum_{i=1}^3 (m \cdot c_p(T))_i dT \\ &= \int_{T_1}^{T_{\text{opt}}} \left[(m \cdot c_p(T))_{\text{EG}} + (m \cdot c_p(T))_{\text{salt}} + (m \cdot c_p(T))_{\text{NH}_3} \right] dT \end{aligned} \quad (7)$$

$$Q_{\text{reheat}} = m_{\text{NH}_3} \cdot (h(T_s) - h(T_{\text{opt}})) \quad (8)$$

$$Q_{\text{input}} = Q_{\text{sen,opt}} + \Delta H_r \cdot \Delta x + Q_{\text{reheat}} \quad (9)$$

$$E_{\text{input}} = \left(1 - \frac{T_a}{T_{\text{opt}}}\right) \cdot (Q_{\text{sen,opt}} + \Delta H_r \cdot \Delta x) + \left(1 - \frac{T_a}{T_s}\right) \cdot Q_{\text{reheat}} \quad (10)$$

When the optimal desorption temperature is lower than the ambient temperature as shown in Fig. 4(c), the potential cooling production can be estimated by Eqs. (11) and (12).

$$\begin{aligned} Q_{\text{ref}} &= \Delta H_r \cdot \Delta x \\ &\quad - \left[(m \cdot c_p(T))_{\text{EG}} + (m \cdot c_p(T))_{\text{salt}} + (m \cdot c_p(T))_{\text{NH}_3} \right] \cdot (T_a - T_{\text{opt}}) \end{aligned} \quad (11)$$

$$E_{\text{ref}} = (T_a/T_{\text{opt}} - 1) \cdot Q_{\text{ref}} \quad (12)$$

The mechanical energy output from the assumed isentropic expansion can be expressed as:

$$W = E_w = m_{\text{NH}_3} \cdot (h_{\text{out}} - h_{\text{in}}) \quad (13)$$

The equations of energy efficiency and exergy efficiency of each energy production are presented as follows, where the subscript 1 and 2 denote the first half-cycle and the second half-cycle, respectively.

$$\eta_{\text{en,w}} = (W_1 + W_2) / (Q_{\text{input1}} + Q_{\text{input2}}) \quad (14)$$

$$\text{COP} = Q_{\text{ref}} / (Q_{\text{input1}} + Q_{\text{input2}}) \quad (15)$$

$$\eta_{\text{ex,w}} = (E_{w1} + E_{w2}) / (E_{\text{input1}} + E_{\text{input2}}) \quad (16)$$

$$\eta_{\text{ex,ref}} = E_{\text{ref}} / (E_{\text{input1}} + E_{\text{input2}}) \quad (17)$$

It is arguable that the overall energy efficiency (first law efficiency) of work output and refrigeration output expressed as Eq. (18) overestimates the efficiency of the cycle by not considering the quality of refrigeration output. To compare different combined power and cooling cycles in a more equitable way, as recommended by literature [23], the energy efficiency was calculated by Eq. (19) in this work. The exergy efficiency of the combined cycle can be calculated by Eq. (20).

$$\eta_{\text{en}} = \eta_{\text{en,w}} + \text{COP} \quad (18)$$

Table 1
Thermodynamic parameters of ammonia and different sorbent salts. [1,24].

	ΔH_r J/mol	ΔS_r J/(mol K)	Max. Uptakes g(NH ₃)/g(salt)	^a c_p J/(kg K)
NH ₃	23366	150.52	–	–
MnCl ₂ (2–6 NH ₃)	47416	228.07	0.540	$\frac{4.184}{M_{\text{MnCl}_2}} \times (16.2 + 0.0052 \times T(\text{K}))$
NaBr (0–5.25 NH ₃)	30491	208.8	0.867	$\frac{4.184}{M_{\text{NaBr}}} \times (11.74 + 0.00233 \times T(\text{K}))$
SrCl ₂ (1–8 NH ₃)	41431	228.8	0.751	$\frac{4.184}{M_{\text{SrCl}_2}} \times (18.2 + 0.00244 \times T(\text{K}))$

^a M is the molecular mass, g/mol.

$$\eta_{\text{en}} = \eta_{\text{en,w}} + \frac{E_{\text{ref}}}{Q_{\text{input1}} + Q_{\text{input2}}} \quad (19)$$

$$\eta_{\text{ex}} = \eta_{\text{ex,w}} + \eta_{\text{ex,ref}} \quad (20)$$

4. Results and discussions

4.1. The optimal desorption temperature and work output

Fig. 5 shows the work output on the basis of 1.0 kg reacted ammonia. The work output using different sorbent pairs in the first half RPG cycle are shown in Fig. 5(a), (c) and (e) under different heat source temperature and different desorption temperature; the work output in the second half-cycles are shown in Fig. 5(b), (d) and (f). According to thermodynamic equilibrium and mono-variant characteristics of HTS and LTS ammoniates, the first half-cycle requires higher heat source temperature to trigger desorption of HTS ammoniates, drive vapour expansion and residually provide enough adsorption pressure for LTS ammoniates. The threshold of such a desorption temperature for effective work output is at around 120 °C for MnCl₂–NaBr pair, and around 70 °C for the other two pairs. Contrastingly, the desorption temperature in the second half-cycles can be sub-zero level because the LTSs have comparatively higher desorption pressure and the HTSs have lower adsorption pressure, that indicates much larger pressure difference favourable for power generation than that in the first half-cycle.

The single red curve marked as “basic process without reheating” lying at the bottom in each figure represents the original basic RPG cycle, namely, the available heat source is directly used for desorption. A series of black curves topping on the red curve imply the potential improvement by introducing reheating process, as each black curve represents the varying work output as ammonia is desorbed at lower temperature and subsequently reheated to the given heat source temperature. The work output increases with the raising desorption temperature firstly, which is caused by the enlarging pressure difference between desorption and adsorption, respectively located at the upstream and downstream of the expander. Afterwards, if the heat source temperature is sufficiently high, the work output curves reach their vertex followed by downward tendency as desorption temperature continuously rises. In this instance, apparently the optimal desorption temperature for the maximum work output appearing as the vertex is lower than the given heat source temperature; otherwise the given heat source temperature is reckoned as the optimal desorption temperature. The reason for the decreasing part of work output curves is mainly attributed to the constraint of ammonia saturation condition. It is reflected in Fig. 3 that the ammonia saturation line, SrCl₂–NH₃ and NaBr–NH₃ reaction equilibrium lines tend to aggregate as the temperature rises, i.e. the state of the desorbed ammonia is getting closer to the saturation state, leading to narrowing space for dry vapour expansion and therefore less work output. The optimal HTS desorption temperature are mainly higher than 100 °C while for LTS desorption it is mostly no higher than 60 °C, as can be seen from Fig. 5. It is noted that in the second half-cycles, as the desorption temperature continues climbing the work output reach their individual valley bottom but then tend to bounce back and start escalating. That is because the desorbed ammonia enters the super-critical domain at some point around the valley, which implies more potential of vapour expansion beyond the saturation condition.

Since the expansion of the ammonia desorbed by LTS is more heavily limited by the saturation than that desorbed by HTS, the implementation of reheating leads to more prominent improvement in the second half-cycles than the first half-cycles as shown in Fig. 5. For example, the maximum work output in the first half-cycle is increased by 2–200% depending on different sorbent

pairs when the heat source temperature is at 200 °C, while the maximum work output in the second half-cycles is improved by 500–600%.

(1) Basic RPG cycle

Fig. 6 shows the pressure ratio of basic RPG cycle using different sorbent pairs. The pressure ratios in the first half-cycles are much lower than those in the second half-cycles at any desorption temperature, as those values in the second half-cycles all soar to the magnitude of hundreds as the desorption temperature reaching around 100 °C. However, the actual expansion ratios of RPG cycles shown in Fig. 7 are much lower. It should be noted that the different interpretation of the ‘pressure ratio’ and the ‘expansion ratio’ in this work as the former one represents the external condition that may favour or limit the vapour expansion, and the later one reflects the actual thermodynamic state evolution of the working fluid undertaking vapour expansion.

Ideally, larger pressure ratio is favourable for productive generation through vapour expansion, as long as the dry expansion can be guaranteed and the expander can handle such expansion ratio. Although the pressure ratios in the first half-cycles are much less than those in the second half-cycles, the expansion ratios in the first half-cycles surpass those in the second half-cycles for most cases, resulting in comparatively productive power generation in the first half-cycles. The key reason for this opposite phenomenon is again the limitation of the ammonia saturation condition, which is clearer if observing from the P–T and T–S diagram: the curve of the ammonia vapour desorbed from LTS ammoniate is closer to the ammonia saturation curve, therefore even though the external condition favours the vapour expansion, the nature of wet fluid limits the expansion, resulting in wasting the majority potential of power generation unless a two-phase expander is used. The ammonia desorbed from HTS ammoniate is relatively distant from the ammonia saturation curve, so there is more space to conduct vapour expansion despite of comparatively smaller pressure ratio.

(2) Advanced RPG cycle with reheating

In Fig. 7(a), the expansion ratio improvement by using reheating can be only achieved at high heat source temperature in the first half-cycle, because the main restriction is the backpressure when at low heat source temperature then it becomes the saturation condition for high temperature heat source, and the reheating concept targets the later one. The expansion ratio improvement is more distinctive in the second half-cycle, as shown in Fig. 7(b), it is improved from around 5 or even less up to few tens. The optimal expansion in many cases ideally ends at the intersection point of ammonia saturation line and backpressure line, as the end point of the bottom left hand side of the grey region shown in Fig. 3, therefore there is overlap between some curves in Fig. 7 which use the same salt ammoniate at the downstream of the expander so that both the backpressure line and ammonia saturation line are fixed which yields the same optimal expansion process when with the same heat source.

Some optimal desorption temperatures in advanced RPG cycle are substantially lower than the ambient temperature, as shown in Fig. 5(d) and (f) (the dashed line in the figure denotes ambient temperature), especially for the case using MnCl₂–NaBr pair, the optimal desorption temperature is from –28 °C to 9 °C when the heat source temperature is between 25 °C and 200 °C. That suggests the potential of considerable cooling product through the LTS desorption as well as achieving the maximum work output after reheating process. In other words, with one desorption heat input in the first half-cycle and two small sensible heat input for reheating in each half-cycle, an advanced RPG cycle can harvest

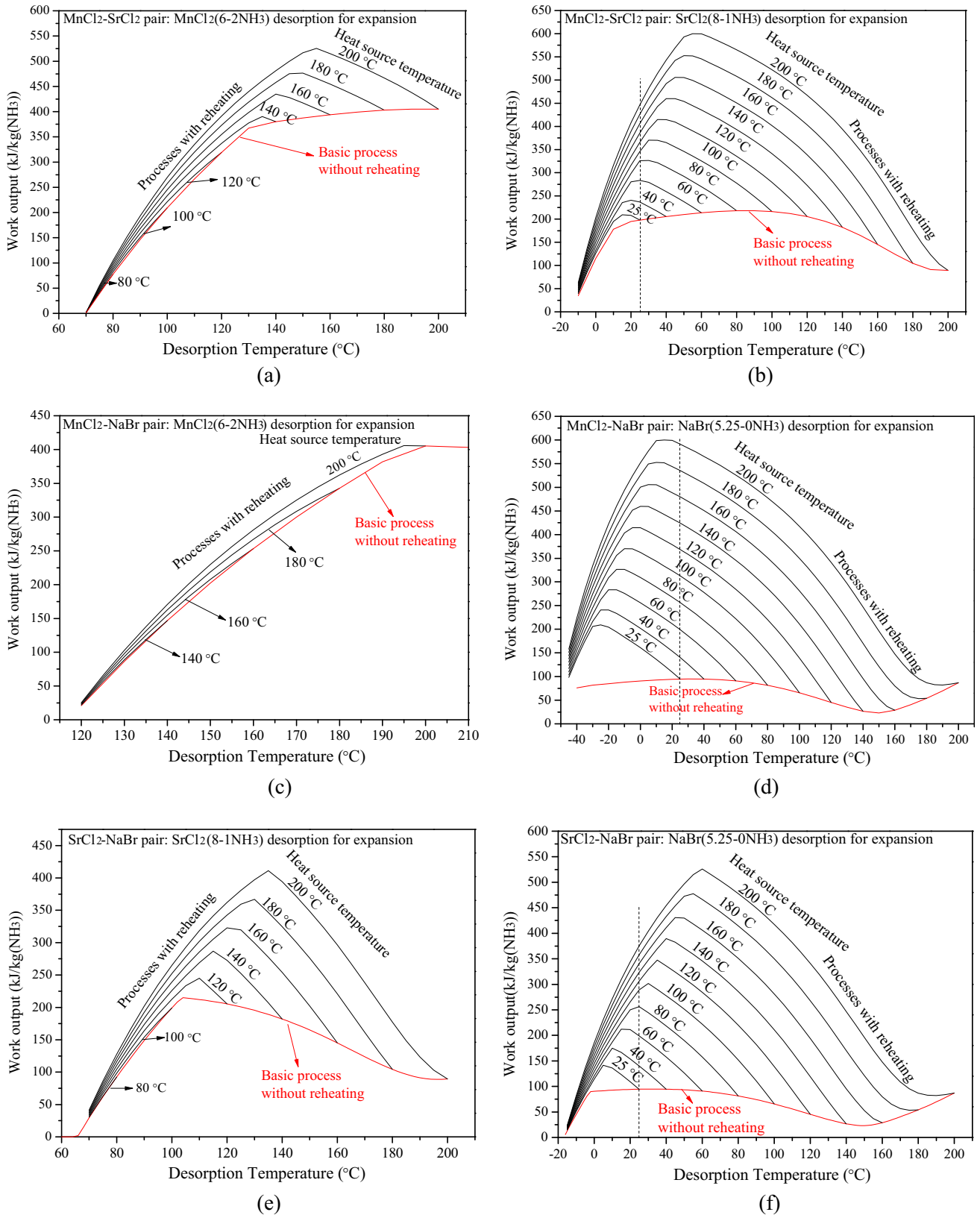


Fig. 5. Work outputs of RPG cycles with different sorbent pairs under conditions of different desorption temperature and reheating temperature.

two work outputs and a big chunk of cooling energy. Additionally, it is noteworthy the distinction between the proposed advanced RPG and the resorption power and cooling cogeneration cycle reported in reference [12]: (1) the present cycle acquires one more work output in the second half-cycle. (2) A reheating process is uti-

lised on the basis of the identification of the optimal desorption temperature to achieve maximum work output. The reheating process is selective and applicable for both first and second half-cycles, therefore it can continuously recover waste heat and have higher energy utilisation efficiency.

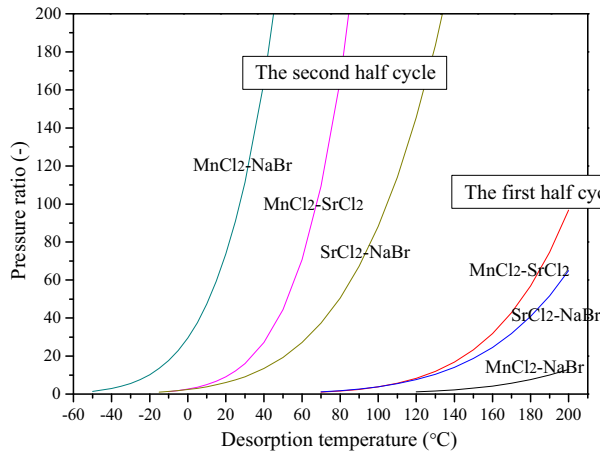


Fig. 6. Pressure ratio of RPG cycles using different sorbent pairs at different desorption temperature.

Fig. 8 clearly depicts the maximum potential and the prominent superior of the advanced RPG cycle compared to basic RPG cycle under different operational conditions. Generally, the reheating concept improves the total work output in a complete operation cycle by 10–600%, depending on sorbent pairs and heat source temperature. Once the heat source temperature is higher than the optimal desorption temperature, the work output appears to linearly elevate with the heat source temperature. The $\text{MnCl}_2\text{-SrCl}_2$ pair is superior to other two sorbent pairs for specific power generation capacity under the studied conditions, which can produce 540 kJ/kg (NH_3) work in the first half-cycle and about 600 kJ/kg work in the second one when the heat source temperature is at 200 °C.

4.2. Thermal efficiency, exergy efficiency and energy density

Apparently, more work output in advanced RPG cycle leads to higher system efficiencies. Moreover, the efficiencies are improved further because of less sensible heat consumed by the solid adsorbents due to the lower desorption temperature in advanced RPG cycles. Therefore, for the calculation of the Eqs. (14) and (16), the collective effect of the numerator increase and the denominator decrease is that the final efficiency value substantially goes up. The evaluation in this work has not taken the sensible heat load

of metallic reactor into account, otherwise the efficiency improvement by using the advanced cycle can be more evident.

Fig. 9 plots the thermal efficiency and exergy efficiency of power generation, when both half-cycles use the same heat source so as to emulate the continuous recovery of the given low grade heat for quasi-continuous work output. The thermal efficiency of work output based on the advanced RPG cycle is from about 6–24% when the heat source temperature is between 70 °C and 200 °C, that is about 41–63% of the Carnot cycle efficiency. The work output by using $\text{MnCl}_2\text{-NaBr}$ pair is not the highest as shown in Fig. 8, but this sorbent pair has the best work output thermal efficiency as shown in Fig. 9(a), which is reasonable since the optimal desorption temperatures at its second half-cycle are all lower than the ambient temperature so that this portion of desorption heat can be treated as negligible. The exergy efficiency is from about 50–85% depending on different sorbent pairs. Compared to the basic RPG cycles, the thermal efficiency of the advanced RPG cycle is increased by 1.4, 2.0 and 4.6 times and the exergy efficiency is boosted by 2.9, 2.0 and 8.3 times, respectively for $\text{MnCl}_2\text{-SrCl}_2$, $\text{MnCl}_2\text{-NaBr}$, and $\text{SrCl}_2\text{-NaBr}$ pair when the heat source temperature is at 200 °C.

If the desorption occurs at the sub-ambient temperature, the advanced APG cycle can not only just realise the further reduction of energy input but also acquire additional cooling energy. Table 2 representatively shows the efficiencies of advanced RPG cycles which have combined power and cooling outputs using the optimal desorption temperature. The shares of cooling output and work output can be balanced according to the bespoke requirement by adjusting the operating conditions, e.g., the work output could be compromised to reach lower refrigeration temperature. The total energy efficiency (η_{en}) discussed in this work takes the energy quality into consideration as expressed in Eq. (19), the exergy efficiency value associated with the additional cooling output instead of the COP value is used to evaluate the overall efficiency together with the work output thermal efficiency. That is the reason why the η_{en} value is higher than the work output efficiency ($\eta_{\text{en,w}}$) but much lower than the simple sum of the $\eta_{\text{en,w}}$ value and the COP value.

The mechanical energy density of RPG cycle using different sorbent pairs is presented in Table 3, which is defined as the amount of mechanical energy generated by one cycle per unit volume of the sorbent materials. Since the focus of the present work is put on the cyclic thermodynamic optimisation and the maximum potential exploration to provide more generic information, no

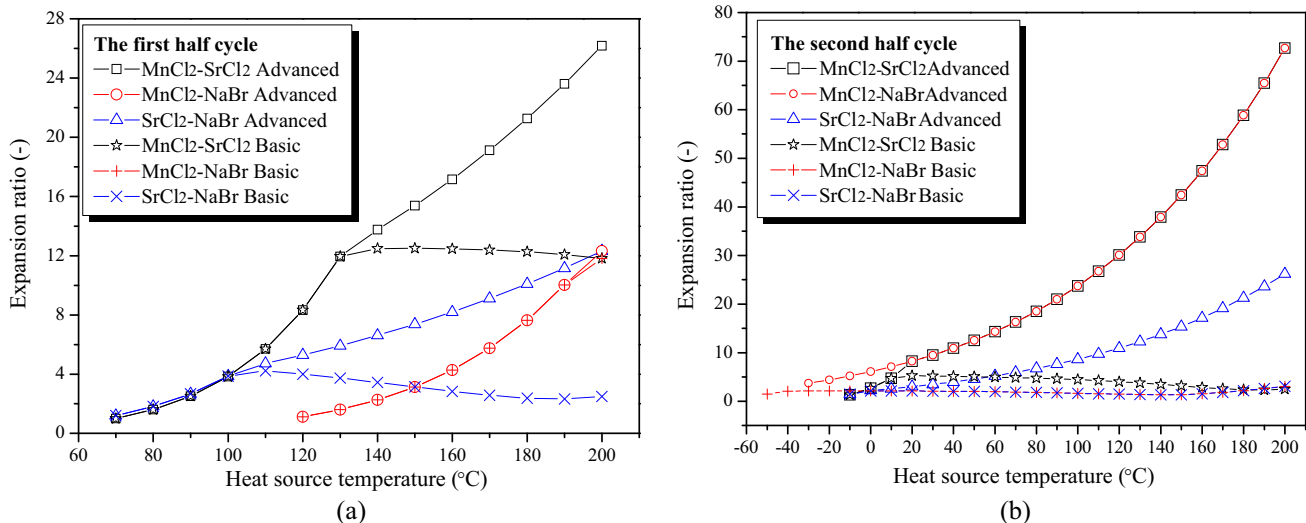


Fig. 7. Expansion ratio of the basic RPG cycles and the advanced RPG cycles (a) in the first half-cycle; (b) in the second half-cycle.

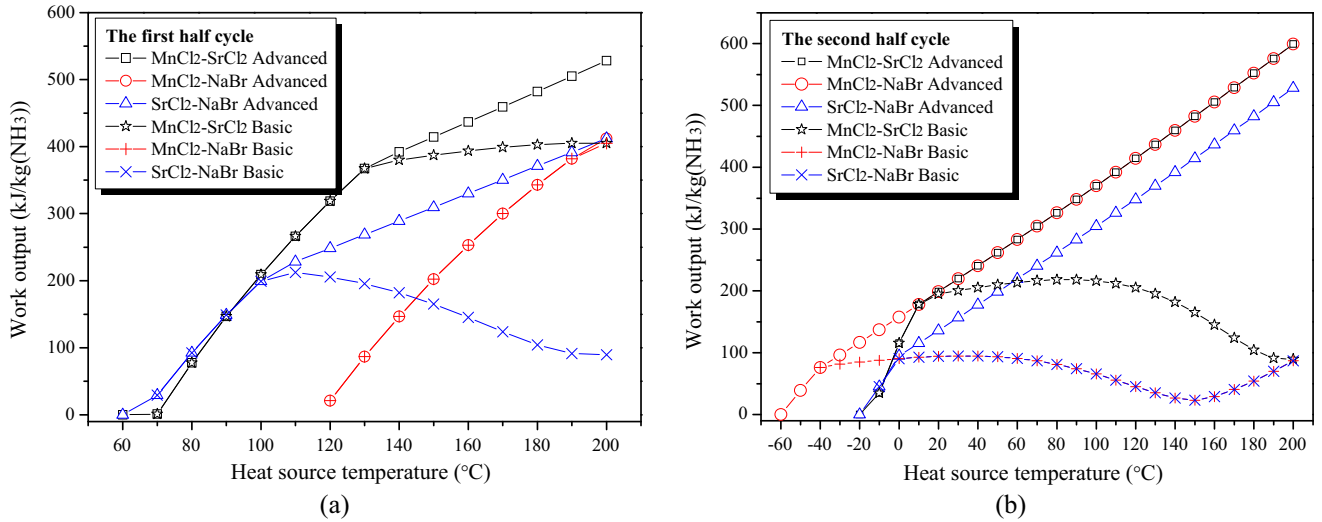


Fig. 8. Work output in basic RPG cycles and advanced RPG cycles, (a) the first half-cycle; (b) the second half-cycle.

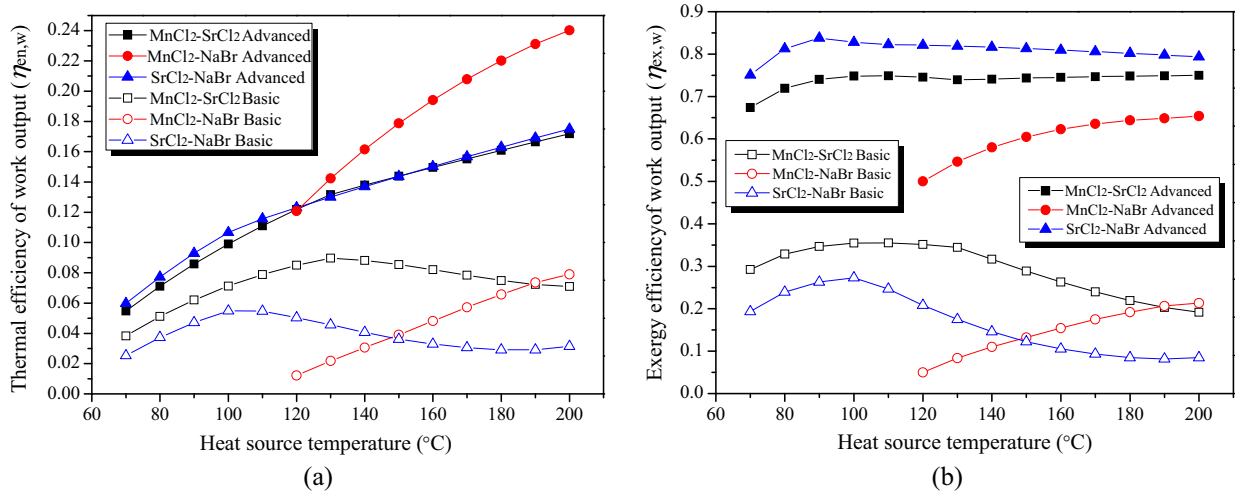


Fig. 9. Work output efficiencies of the basic RPG cycles and the advanced RPG cycles, (a) thermal efficiency; (b) exergy efficiency.

Table 2
Performance of advanced RPG cycles for combined power and cooling output.

Adsorbent pairs	Heat source temperature in first half-cycle (°C)	LTS desorption temperature (refrigeration temperature) (°C)	Reheating temperature (in second half-cycle) (°C)	Work generation efficiency ($\eta_{en,w}$)	COP (refrigeration)	Total energy efficiency (η_{en})	Total exergy efficiency (η_{ex})
MnCl ₂ -SrCl ₂	180	0	80	0.169	0.623	0.226	0.791
	180	10.5	80	0.195	0.628	0.228	0.790
MnCl ₂ -NaBr	180	-20	120	0.173	0.420	0.247	0.740
	180	-10	120	0.188	0.451	0.248	0.741
	180	0	80	0.169	0.478	0.213	0.637
	180	10	80	0.165	0.490	0.191	0.570

Table 3
Mechanical energy density with different sorbent pairs based on one complete cycle.

	Basic RPG cycle (MJ/m ³)	Advanced RPG cycle (MJ/m ³)
MnCl ₂ -SrCl ₂	3.7–52.6	30.1–120.0
MnCl ₂ -NaBr	4.4–55.3	24.7–113.7
SrCl ₂ -NaBr	6.2–24.2	37.0–128.9

specific reactor design nor heat exchanger design is taken into consideration for this density evaluation. If a complete system prototype design with other essential components is envisaged, using

the volume of the whole prototype for energy density calculation can provide more practical insight, the value of which could be smaller than those shown in Table 3.

4.3. Comparison with other bottoming cycles driven by low grade heat for power generation

With the foregoing discovery of some optimal desorption temperature being lower than the ambient temperature, if the advanced RPG cycle operates solely for power generation and there

is no cooling demand, the desorption in the second half-cycle can be implemented deliberately at ambient temperature to minimize thermal energy input, leading to further improved energy efficiency. Additionally, this approach also simplifies the system configuration and operation. The thermal efficiency of the advanced RPG cycle using such an operation strategy is compared to other bottoming cycles, including organic Rankine cycle (ORC), Stirling cycle and thermo-electric cycle (TE), which have been parametrically investigated in Bianchi et al.'s work [25]. The analytical modelling in Bianchi et al.'s work was based on the following practically reasonable assumptions: (1) the temperature difference between the available heat source temperature and the evaporating temperature of the working fluid was fixed at 50 °C; (2) the heat sink temperature was 15 °C while the condensation temperature of the working fluid was at 33 °C; (3) the expander isentropic efficiency was 75%, while mechanical efficiency was provided at 97%. Fig. 10 compares those three cycles from Bianchi et al.'s work with the present advanced RPG cycle which applies the same analytical assumptions aforementioned. The advanced RPG cycle exhibits its competitiveness and prominently superior performance than Stirling cycle and TE cycle under all the conditions studied. The advanced RPG cycles using $\text{MnCl}_2\text{-SrCl}_2$ pair and $\text{SrCl}_2\text{-NaBr}$ pair have higher thermal efficiency than that of ORC when the heat source temperature is between around 120 °C and 200 °C, especially when the heat source temperature is at about 150 °C the efficiency of the former ones is about 20% larger.

According to the variation in Fig. 10 combined with the theoretical principle, it is reasonable to speculate that: (1) the $\text{MnCl}_2\text{-NaBr}$ advanced RPG cycle can achieve the highest thermal efficiency among these three advanced RPG cycles when the heat source temperature is higher than 250 °C; (2) the sorbent pairs grouped by two salt ammoniates which have closer equilibrium with each other are more likely to obtain the higher thermal efficiency when driven by lower temperature heat source, because such a resorption cycle can create moderate pressure ratio between desorption and adsorption in both half-cycles; (3) the adsorbent pairs grouped by two salt ammoniates which have bigger equilibrium disparity between them tend to have higher thermal efficiency when the heat source temperature is sufficiently high due to the great pressure ratio created in the second half-cycle. Therefore, the proposed advanced RPG cycle can flexibly adopt different adsorbent pairs for various application scenarios. As a fact, there are hundreds of adsorbent salts worth of exploring for low grade heat recovery using this resorption cycles, and the in-depth knowledge and more beneficial

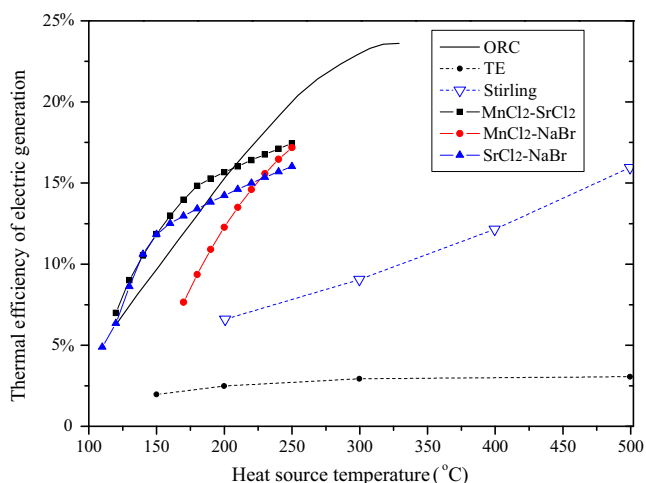


Fig. 10. Comparison of advanced RPG cycles to other bottoming cycles for power generation.

characteristics is to be revealed in the further investigation. Another significant flexibility of the resorption systems is the capability of producing heat-upgrading or refrigeration or power generation or the combination of any of these, which is also certainly appealing and has potential to broadly expand its application.

5. Conclusions

Based on the integrated resorption cycle with a turbine/expander for power generation, an innovative advanced RPG cycle with reheating process was proposed to substantially improve the power output and energy and exergy efficiencies, which can realise continuous waste heat recovery and quasi-continuous power generation. The performance of such an optimised cycle using different sorbent pairs, $\text{MnCl}_2\text{-NaBr}$, $\text{MnCl}_2\text{-SrCl}_2$ and $\text{SrCl}_2\text{-NaBr}$, respectively, were parametrically investigated and compared as the following conclusions can be drawn:

- (1) The proposed reheating process is on the basis of the identification of the optimal desorption temperature, which can mitigate the significant limitation of ammonia being wet fluid and realise productive power generation by maximumly realising the huge pressure ratio created by resorption cycle.
- (2) The work output thermal efficiency by using the advanced RPG cycle is from 6% to 24% when the heat source temperature is between 70 °C and 200 °C, depending on different sorbent pairs; the exergy efficiency is from 50% to 85%, depending on sorbent pairs and heat source temperature. Both efficiencies are greatly improved compared to those of the basic RPG cycle.
- (3) The advanced cycle with $\text{MnCl}_2\text{-NaBr}$ sorbent pair can effectively achieve additional cooling output at temperature from -28 °C to 9 °C with the COP value around 0.4–0.6, and without compromising the optimal work output.
- (4) The analytical comparison showed the competitiveness of the proposed advanced RPG cycle against other bottoming cycles, and the advanced RPG cycle using $\text{MnCl}_2\text{-SrCl}_2$ pair or $\text{SrCl}_2\text{-NaBr}$ pair has higher efficiency than that of ORC when the heat source temperature is in the range of 120–200 °C.
- (5) Considering the variety of adsorption salt pairs, it is worth to continue further parametric and experimental investigations to explore maximum benefits of resorption power generation cycle.

Acknowledgements

The authors gratefully acknowledge the support from the IAA project (Impact Acceleration Account) (EP/K503885/1), IDRIST project (EP/M008088/1) and Heat-STRESS project (EP/N02155X/1), funded by the Engineering and Physical Science Research Council of UK. Data supporting this publication is openly available under an 'Open Data Commons Open Database License'. Additional meta-data are available at: <http://dx.doi.org/10.17634/148532-3>. Please contact Newcastle Research Data Service at rdm@ncl.ac.uk for access instructions.

References

- [1] Wang RZ, Wang LW, Wu JY. Adsorption refrigeration technology: theory and application. China: John Wiley & Sons Singapore; 2014.
- [2] Ziegler F. Recent developments and future prospects of sorption heat pump systems. Int J Thermal Sci 1999;38:191–208.
- [3] Ma ZW, Bao HS, Roskilly AP. Performance analysis of ultralow grade waste heat upgrade using absorption heat transformer. Appl Therm Eng 2016;101:350–61.

- [4] Wu JW, Biggs MJ, Pendleton P, Badalyan A, Hu EJ. Experimental implementation and validation of thermodynamic cycles of adsorption-based desalination. *Appl Energy* 2012;98:190–7.
- [5] Yu N, Wang RZ, Wang LW. Sorption thermal storage for solar energy. *Prog Energy Combust Sci* 2013;39:489–514.
- [6] Maloney JD, Robertson RC. Thermodynamic study of ammonia-water heat power cycles. Oak Ridge National Laboratory Report.CF-53-8-43; 1953.
- [7] Kalina AI. Combined cycle and waste-heat recovery power systems based on a novel thermodynamic energy cycle utilising low temperature heat for power generation. ASME Paper 1983; 83-JPGC-GT-3.
- [8] Zhang XX, He MG, Zhang Y. A review of research on the Kalina cycle. *Renew Sustain Energy Rev* 2012;16:5309–18.
- [9] Goswami DY. Solar thermal power-status of technologies and opportunities for research. In: Jaluria Y, editor. Proceedings of the second ISHNT-ASME heat & mass transfer conference. Suratkal, India: Tata McGraw Hill; 1995. p. 57–60.
- [10] Liu M, Zhang N. Proposal and analysis of a novel ammonia-water cycle for power and refrigeration cogeneration. *Energy* 2007;32:961–70.
- [11] Yu Z, Han J, Liu H, Zhao H. Theoretical study on a novel ammonia-water cogeneration system with adjustable cooling to power ratios. *Appl Energy* 2014;122:53–61.
- [12] Wang LW, Ziegler F, Roskilly AP, Wang RZ, Wang YD. A resorption cycle for the cogeneration of electricity and refrigeration. *Appl Energy* 2013;106:56–64.
- [13] Bao HS, Wang YD, Roskilly AP. Modelling of a chemisorption refrigeration and power cogeneration system. *Appl Energy* 2014;119:351–62.
- [14] Bao HS, Ma ZW, Roskilly AP. Integrated chemisorption cycles for ultra-low grade heat recovery and thermo-electric energy storage and exploitation. *Appl Energy* 2015;164:228–36.
- [15] Mlcak H, Mirolli M, Hjartarson H, Húsavík O, Ralph M. Notes from the north: a report on the debut year of the 2 MW Kalina cycle[®] geothermal power plants in Húsavík, Iceland. *Geothermal Res Council Trans* 2002;26:715–8.
- [16] Macwan S. The Kalina cycle a major breakthrough in efficient heat to power generation. In: CHP 2013 & WHP 2013 Conference and Trade Show. Houston, USA.
- [17] Bao HS, Ma ZW, Roskilly AP. Chemisorption power generation driven by low grade heat – theoretical analysis and comparison with pumpless ORC. *Appl Energy* 2017;186:282–90.
- [18] Lepinasse E, Marion M, Goetz V. Cooling storage with a resorption process. Application to a box temperature control. *Appl Therm Eng* 2001;21:1251–63.
- [19] Vasiliev LL, Mishkinis DA, Antukh AA, Kulakov AG. Resorption heat pump. *Appl Therm Eng* 2004;24:1893–903.
- [20] Jin ZQ, Wang LW, Jiang L, Wang RZ. Experiment on the thermal conductivity and permeability of physical and chemical compound adsorbents for sorption process. *Heat Mass Transfer* 2013;49:1117–24.
- [21] Lu HB, Mazet N, Spinner B. Modelling of gas-solid reaction coupling of heat and mass transfer with chemical reaction. *Chem Eng Sci* 1996;3829.
- [22] Hirata Y, Fujioka K. Thermophysical properties and heat transfer characteristics of CaCl₂ heat pump reactor associated with structural change of reactive salts. V Minsk International Seminar "Heat Pipes, Heat Pumps, Refrigerators", September, 2003, Minsk, Belarus.
- [23] Vijayaraphavan S, Goswami DY. On evaluating efficiency of a combined power and cooling cycle. *J Energy Res Technol* 2003;125:221–7.
- [24] Liley PE. Physical and chemical data. In: Perry RH, Green DW, Maloney JO, editors. Perry's chemical engineers' handbook. New York: McGraw-Hill Companies Inc.; 1999.
- [25] Bianchi B, De Pascale A. Bottoming cycles for electric energy generation: parametric investigation of available and innovative solutions for the exploitation of low and medium temperature heat source. *Appl Energy* 2011;88:1500–9.